

# Gamma-Ray Bursts Black hole accretion disks as a site for the $\nu p$ -process

L.-T. Kizivat,<sup>1,2</sup> G. Martínez-Pinedo,<sup>1</sup> K. Langanke,<sup>1,2,3</sup> R. Surman,<sup>4</sup> and G. C. McLaughlin<sup>5</sup>

<sup>1</sup>*GSI Helmholtzzentrum für Schwerionenforschung, Planckstr. 1, 64291 Darmstadt, Germany*

<sup>2</sup>*Institut für Kernphysik, Technische Universität Darmstadt, 64289 Darmstadt, Germany*

<sup>3</sup>*Frankfurt Institute for Advanced Studies, Ruth-Moufang-Str. 1, 60438 Frankfurt, Germany*

<sup>4</sup>*Department of Physics and Astronomy, Union College, Schenectady, NY 12308*

<sup>5</sup>*Department of Physics, NC State University, Raleigh, NC 27695-8202*

(Dated: November 2, 2018)

We study proton rich nucleosynthesis in windlike outflows from gamma-ray bursts accretion disks with the aim to determine if such outflows are a site of the  $\nu p$ -process. The efficacy of this  $\nu p$ -process depends on thermodynamic and hydrodynamic factors. We discuss the importance of the entropy of the material, the outflow rate, the initial ejection point and accretion rate of the disk. In some cases the  $\nu p$ -process pushes the nucleosynthesis out to  $A \sim 100$  and produces light p-nuclei. However, even when these nuclei are not produced, neutrino induced interactions can significantly alter the abundance pattern and cannot be neglected.

PACS numbers: 26.30.-k, 25.30.Pt, 97.60.Bw

## I. MOTIVATION AND METHODS

Burbidge, Burbidge, Hoyle and Fowler [1] and independently Cameron [2] have proposed three major nucleosynthesis processes - the r-, s-, and p-process - to make nuclei heavier than iron in stars. Since this pioneering work impressive progress has been achieved in the understanding of these processes [3]. Nevertheless important questions still remain unanswered like the definite astrophysical site of the r-process [4] and the mechanism responsible for the production of light p-nuclei [5].

Neutrino-driven winds from core-collapse supernovae are considered as a site for the production of light p-nuclei. In this scenario, light p-nuclei can be produced by different mechanisms. Slightly neutron rich outflows with electron fractions  $Y_e \approx 0.48$  result in the production of light p-nuclei with  $A \leq 92$ , i.e.  $^{74}\text{Se}$ ,  $^{78}\text{Kr}$ ,  $^{84}\text{Sr}$ , and  $^{92}\text{Mo}$  [6]. The production of some of these nuclei and in particular  $^{92}\text{Mo}$  is enhanced by neutrino captures on nuclei with  $N \approx 50$  [7]. Light-p nuclei, including  $^{94}\text{Mo}$  and  $^{96,98}\text{Ru}$ , can be produced in proton-rich outflows via the  $\nu p$ -process [8–10]. It is this latter mechanism that we focus on in this paper. It operates in proton-rich environments with high neutrino and antineutrino fluxes as are found in the early ejected matter in core-collapse supernovae. Here the matter is ejected from the surface of the nascent neutron star as free nucleons. The competition of neutrino captures on neutrons and antineutrino captures on protons drives the matter proton-rich as both neutrino types have rather similar luminosities and the average antineutrino energy is not large enough compared to the neutrino energy to compensate for the difference in reaction Q-values. Upon reaching cooler regions, i.e. with increasing distance from the neutron star surface, the nucleons assemble in nuclei and, without further neutrino reactions, the proton-rich matter freezes out with a significant production of  $N = Z$  nuclei like  $^{56}\text{Ni}$  and  $^{64}\text{Ge}$  and some free protons left. However, antineutrino captures on these protons ensure a significant

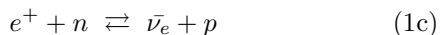
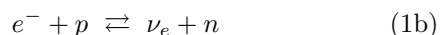
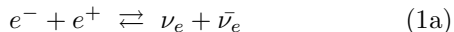
presence of free neutrons which can be captured on the  $N = Z$  nuclei via  $(n, p)$  and  $(n, \gamma)$  reactions allowing for matter flow beyond  $^{56}\text{Ni}$  and  $^{64}\text{Ge}$  which otherwise with their long halflives against proton capture and beta decay could not be overcome during the dynamical timescale of supernova nucleosynthesis (a few seconds). Different studies of the  $\nu p$ -process [8–10] have shown that it can produce light p-nuclides in abundances which might be sufficient to explain their observed solar values. It is expected that the ejection of some proton-rich matter in the presence of strong antineutrino fluxes is a general feature of core-collapse supernovae making the occurrence of the  $\nu p$ -process a general supernova phenomenon.

Recent studies indicate that quite similar physical conditions, like those which give rise to the  $\nu p$ -process in supernovae, also occur in the windlike outflows from the accretion disk surrounding a black hole featuring a gamma-ray burst. Considerable observational evidence now connects long duration gamma ray bursts with the collapse of massive stars. McFadyen and Woosley [11] pioneered a currently widely used model for these events: a collapse of massive star with  $M > 25 M_\odot$  ( $M_\odot$  denoting our sun's mass) fails to produce a standard core collapse supernovae with a neutron star at the center, and instead produces an accretion disk surrounding a black hole. Here again, the temperature in the disk is sufficiently high so that matter is ejected as free nucleons. Furthermore, the ejection occurs in the presence of quite sizable neutrino fluxes [12] Depending on the matter accretion rate of the black hole disk, neutrinos and antineutrinos can get trapped defining neutrino surfaces from which they decouple from the disk matter [12, 13]. It is found that disks with moderate accretion rates (around  $1 M_\odot \text{ s}^{-1}$ ) have neutrino and antineutrino fluxes which drive the ejected matter proton-rich making the occurrence of the  $\nu p$ -process an exciting possibility [14]. Lacking detailed (magneto)hydrodynamic models of the ejection, the amount of proton-rich ejecta can be estimated to reach up to  $0.01 M_\odot$  according to the analytical outflow

model of ref. [15] and typical disk parameters. A broad survey of nucleosynthesis from GRB accretion disks indicated that some p-process elements may be formed this way [16], but a study of the  $\nu p$ -process mechanism has not been undertaken. It is the aim of this paper to study this intriguing possibility. Our study is based on the temperature, density, electron-to-nucleon ratios profiles and dynamical expansion times of the windlike outflows as described by McLaughlin and Surman [12, 16]. The respective wind trajectories are then coupled to an extensive nuclear network.

## II. MODEL

The disks studied in this work are all based on the model of Neutrino-Dominated-Accretion-Flows, “NDAF’s” [17]. Two NDAF-based disk models are used and results compared. The models labeled A1–A6 are from a disk model by T. DiMatteo, R. Perna and R. Narayan [18]; this model was the first to incorporate the effects of neutrino trapping. The models labeled B1–B5 are from a fully relativistic disk model by W.-X. Chen and A.M. Beloborodov [19] that additionally incorporates improved microphysics, including the influence of electron degeneracy and an evolving neutron-to-proton ratio. For a detailed description of neutrino-cooled accretion disks, see [18], [17], [19]. Radial profiles for the disk density  $\rho$ , temperature  $T$ , disk scale height  $H$ , nuclear composition and neutrino and antineutrino luminosity  $L_{\nu, \bar{\nu}}$  are found to depend strongly on the accretion disk parameters, i.e., the disk accretion rate  $\dot{M}$ , viscosity parameter  $\alpha$ , black hole spin  $a$  and accretion disk mass  $M$ . The matter in the disk has to decrease its internal energy to be accreted into the black hole. This cooling of the disk proceeds either through advection or neutrino emission [19]. Cooling through neutrino emission only becomes important in regions where the temperature and density are sufficiently high for the below reactions to occur with significant rates:



These neutrinos emitted from the disk interact with material ejected from the disk, influencing the subsequent nucleosynthesis in the outflow. The neutrino and antineutrino fluxes above the disk are calculated as in Surman and McLaughlin [12]. Where the disk is optically thin to neutrinos and antineutrinos, the emitted neutrino fluxes are determined from the rates of the above reactions. In the inner regions of the disk, first the neutrinos and then the antineutrinos become trapped. Here we determine the surfaces at which electron neutrinos and antineutrinos decouple vertically from the accretion disk and then use the local disk temperatures at these places

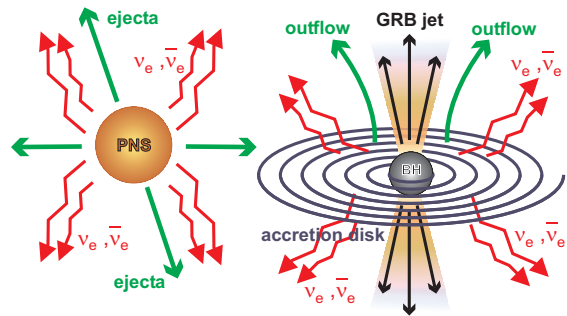


FIG. 1: (Color online) Scheme of the geometry in core collapse supernovae and GRB accretion disks. “PNS” is the nascent proto-neutron star. Neutrinos and matter in the early ejecta are emitted radially. “BH” denotes the black hole, the central engine in a GRB accretion disk. The outflows leave the disk vertically.

to adjust the temperatures of the neutrino and antineutrino fluxes leaving the disk.

The evolutionary path of mass elements in an outflow is given in a trajectory. The initial thermodynamic parameters of the matter in the outflow are set by the characteristics of the disk, i.e. vary according to the disk model used. Matter in the outflows leaves the disk in perpendicular direction to the disk. Close to the disk a treatment in cylindrical symmetry is convenient. With increasing distance to the disk a transition from cylindrical to spherical symmetry is appropriate.

The present calculations are based on the simulations of the windlike outflows of Surman and McLaughlin [14]. Using the method outlined in [14] we construct parametrized trajectories which describe the ejection of mass elements from the disk. Due to the rather high temperatures the matter is originally ejected as free neutrons and protons and the proton-to-neutron ratio is set by weak interactions due to the strong neutrino and antineutrino fluxes which occur rather close to the neutrino surfaces. Upon reaching cooler regions at distances noticeably further out than these surfaces nucleons can re-assemble to nuclei. This nucleosynthesis process in the matter outflow we describe by an extensive nucleosynthesis network subject to the thermodynamical conditions of the outflowing matter.

We assume the outflows to be adiabatic defined by the entropy per baryon  $S$  in units of  $k_B$ . A second crucial parameter is the velocity of the ejected matter as a function of distance  $R$  from the black hole in the center of the disk. This velocity  $u$  is parameterized as

$$|u| = v_\infty \left(1 - \frac{R_0}{R}\right)^\beta. \quad (2)$$

where  $R_0$  is the radius at which the outflow leaves the accretion disk (see Figure 1),  $v_\infty$  is the asymptotic velocity of the matter (assumed to be  $3 \times 10^4$  km/s) and the parameter  $\beta$  determines the acceleration of the outflow and therefore is referred to as “acceleration param-

eter” [14]. The parameter  $\beta$  is important as it defines the time the outflow is subjected to weak interactions in the strong neutrino fluxes. Large values of  $\beta$  correspond to slowly accelerating outflows with rather long neutrino interaction times, while small  $\beta$  values define outflows with fast accelerations and hence less time for neutrino interactions.

As pointed out in [14] the electron fraction  $Y_e$  of the ejected matter depends also critically on the rate by which the black hole accretes matter to the disk. Typical values are in the range  $0.01\text{--}10 M_\odot \text{ s}^{-1}$  [17]. Disks with smaller accretion rates of order  $0.1 M_\odot \text{ s}^{-1}$  and  $1 M_\odot \text{ s}^{-1}$ , as explored in our current work, are found to have only small regions of trapped neutrinos in the disk and even smaller ones for antineutrinos. Under such conditions there are relatively few antineutrinos interacting with the matter outflow, while neutrino captures on neutrons are still sizable. For such low accretion rates the weak interaction will drive the outflowing matter proton-rich [14] with free protons available making it a tempting site for  $\nu p$ -process nucleosynthesis. It is exactly these conditions which we will study in the following.

We note that for even smaller accretion rates neither neutrino nor antineutrino trapping occurs and the free proton fraction in the ejected matter is not significant. Such an environment is not favorable for  $\nu p$ -process nucleosynthesis.

Our nucleosynthesis network considers 3347 nuclei covering the nuclear chart from protons and neutrons to  $^{211}\text{Eu}$ . The appropriate reaction rates among these nuclei mediated by the strong and electromagnetic interaction are taken from the reaction library [20]. Weak-interaction rates for nuclei are adopted from Zinner [21]. However, we find that only neutrino reactions with free protons and neutrons have influence on the nucleosynthesis process. The network has been numerically solved as outlined in [22, 23].

### III. RESULTS

As outlined above we expect that the nucleosynthesis in the accretion disk outflows depends on the parameter values for the mass accretion rate  $\dot{M}$ , the acceleration parameter  $\beta$ , the radius  $R_0$  at which the matter decouples from the disk and the entropy in the outflow  $S$ . Furthermore, the proton-to-neutron ratio of the ejected matter is crucial for the nucleosynthesis. As this ratio is set by weak interaction processes close to the neutrino surfaces it is expected to be different for the neutrino-dominated accretion disk models of DiMatteo et al. [18] and of Chen and Beloborodov [19] which predict quite noticeable differences in the relative neutrino and anti-neutrino fluxes and spectra. Hence we have performed a set of nucleosynthesis calculations for both models varying the parameters  $\dot{M}$ ,  $\beta$ ,  $R_0$  and  $S$ . The chosen parameter values for the various models which we studied in details are defined in Table I, where the labels ‘A’ and ‘B’ refer to

model	$\dot{M}$ ( $M_\odot \text{ s}^{-1}$ )	$R_0$ (km)	$\beta$	$S$ ( $k_B$ )
A1 & B1	1	100	2.5	30
A2 & B2	1	100	0.8	30
A3 & B3	1	100	2.5	15
A4 & B4	1	100	2.5	50
A5	1	250	2.5	50
B5	1	50	2.5	50
A6	0.1	100	2.5	30

TABLE I: Parameter values for the various studied models.

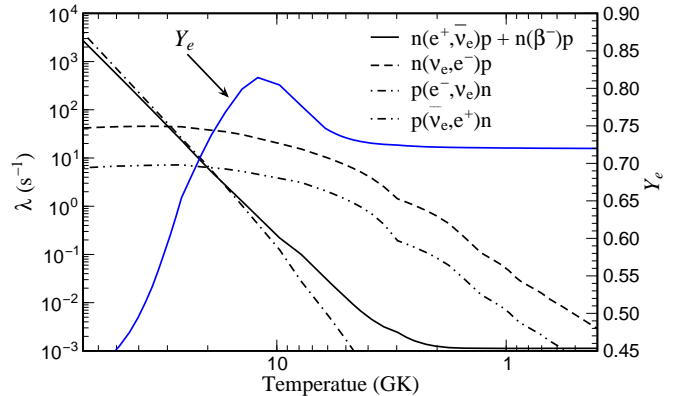


FIG. 2: (Color online) Model A1: Evolution of the capture rates for positrons (solid line) and neutrinos (dashed) on neutrons and for electrons (dashed-dotted) and antineutrinos (dashed-dotted-dotted) on protons as a function of the matter temperature. Notice that the rate for positron capture on neutrons includes also the neutron beta decay rate. The evolution of the electron fraction,  $Y_e$  is also shown (right y-scale). Temperature is measured from the moment matter decouples from the disk where it is still strongly neutron-rich.

the disk models of [18] and [19], respectively.

We start with nucleosynthesis studies for the outflows from the disk model of DiMatteo *et al.* [18]. The Model A1 with the modest accretion rate  $\dot{M} = 1 M_\odot \text{ s}^{-1}$  and relatively slow outflow velocities corresponds to conditions for which one expects the outflows to be proton-rich as at the radius  $R_0$  at which matter is expelled from the disk (100 km) the disk is dense and hot enough for neutrino producing reactions (Eq. 1) to occur with significant rates. Figure 2, shows the time evolution of the electron fraction  $Y_e$  and the capture rates of positrons and neutrinos on neutrons and electrons and antineutrinos on protons. Time is measured from the moment matter decouples from the disk where it is still strongly neutron-rich and consists of free protons and neutrons. Their ratio, however, is changed due to fast electron-positron captures and interactions with the large neutrino and antineutrino fluxes. Importantly the neutrino fluxes are about one order of magnitude larger than those for antineutrinos, while the average energy of antineutrinos is around 2 MeV larger than the one of neutrinos. As

a consequence neutrino captures on neutrons dominate and drive the composition proton-rich and a peak value of  $Y_e \sim 0.8$  is reached. The increase in  $Y_e$  is stopped, once alpha particles form which use up all available neutrons. Due to the high particle thresholds of  ${}^4\text{He}$  neutrons are then protected against neutrino interactions, while the remaining free protons are still subject to strong antineutrino fluxes. Continuing antineutrino captures on protons supply more neutrons, which, in an “inverse” alpha effect [7, 24, 25] are combined with additional protons into more  ${}^4\text{He}$ . As a consequence of these antineutrino captures the  $Y_e$  value decreases. At  $T \sim 3$  GK the weak interaction rates have decreased sufficiently as the neutrino fluxes decrease with distance and the matter composition freezes out with a  $Y_e$  value around 0.72. Starting with the triple-alpha reaction a network of reactions (called alpha process [26, 27]) produces heavier nuclei, which can become the seed for additional nucleosynthesis, and reduces the abundance of  ${}^4\text{He}$ . For conditions with  $Y_e > 0.5$ , the seeds consist mainly of  $N = Z$  nuclei with multi-alpha structures like  ${}^{56}\text{Ni}$ ,  ${}^{60}\text{Zn}$ ,  ${}^{64}\text{Ge}$ , with an abundance of free protons  $Y_p = 2Y_e - 1$  [9]. The long halfives of these seed nuclei against beta decay and proton capture would stop the nucleosynthesis flow, if it were not for the continuous supply of free neutrons produced by antineutrino captures on the protons. This is the key element of the  $\nu p$ -process. Indeed a sequence of  $(n, p)$  and  $(p, \gamma)$  reactions allows for synthesis of elements upto the mass range  $A \sim 80 - 100$  for the conditions of model A1, as can be seen in Fig. 3. As a comparison we also show the abundance distribution obtained with the same nucleosynthesis network, however, switching off the neutrino and, importantly, antineutrino capture reactions once the freeze-out value of  $Y_e$  is reached. Strikingly the matter flow stops at the alpha seed nuclei with long halfives (e.g.  ${}^{56}\text{Ni}$ ,  ${}^{60}\text{Zn}$ ..) as in this scenario no free neutrons are available to carry the matter flow to larger mass numbers as it is guaranteed in the  $\nu p$ -process due to the late-time neutrons produced by antineutrino captures on protons.

We have seen that model A1 allows for a substantial  $\nu p$ -process to occur. The outflow model A2 is identical to model A1, except that it has a faster acceleration (smaller  $\beta$  value). Thus, although the neutrino and antineutrino luminosities are the same as in model A1, the ejected matter has shorter time to interact with neutrinos and consequently the neutrino fluence is much smaller. While in model A1 the neutrino fluence in the temperature range 3–1 GK is  $4 \times 10^{38} \text{ cm}^{-2}$  (a value similar to the one used in  $\nu p$ -process nucleosynthesis studies in supernova environments [8, 9]) the value for model A2 is only  $10^{37} \text{ cm}^{-2}$ . Consequently, model A2 is expected to show only a rather weak  $\nu p$ -process which is indeed borne out by our nucleosynthesis calculation, as can be seen in Fig. 4.

Another important parameter, which affects the matter composition and the subsequent nucleosynthesis, is the entropy  $S$ . In general the larger the entropy, the

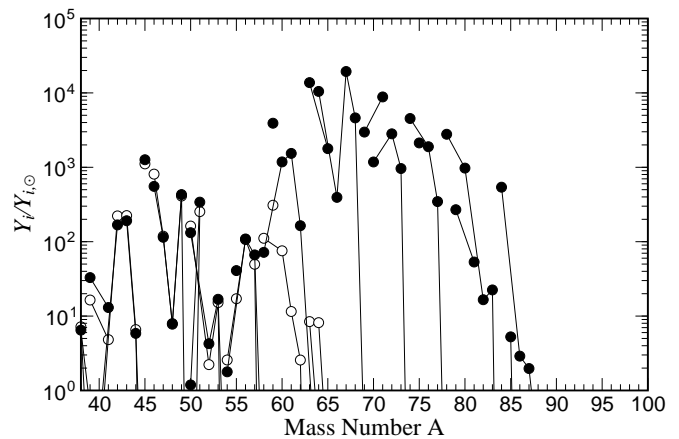


FIG. 3: Final isotopic abundances (solid circles) for the nucleosynthesis calculations in disk model A1 relative to solar abundances [28]. The empty circles show the abundances obtained with the same nucleosynthesis network, however, switching off neutrino and anti-neutrino capture reactions once the freeze-out value for  $Y_e$  is reached.

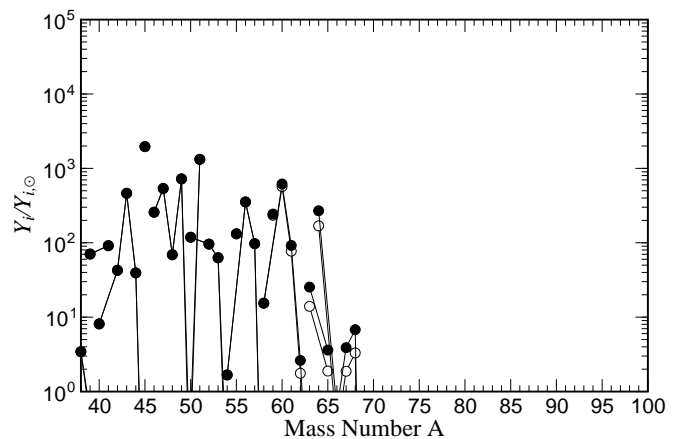


FIG. 4: Same as Fig. 3, but for model A2.

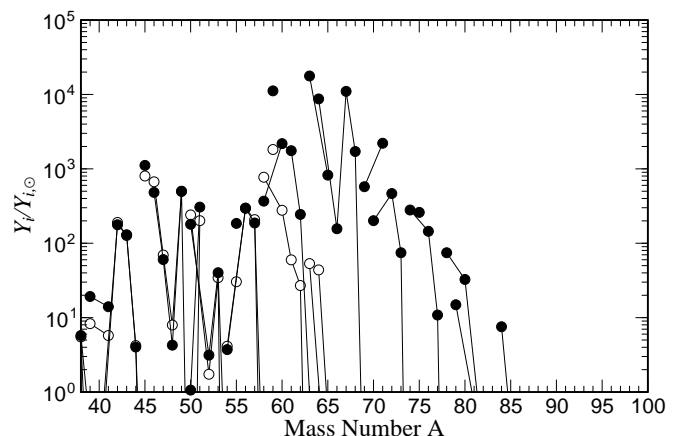


FIG. 5: Same as Fig. 3, but for model A3.

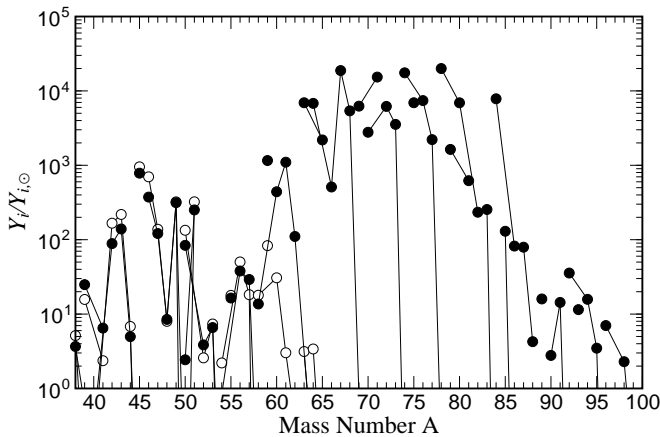


FIG. 6: Same as Fig. 3, but for model A4.

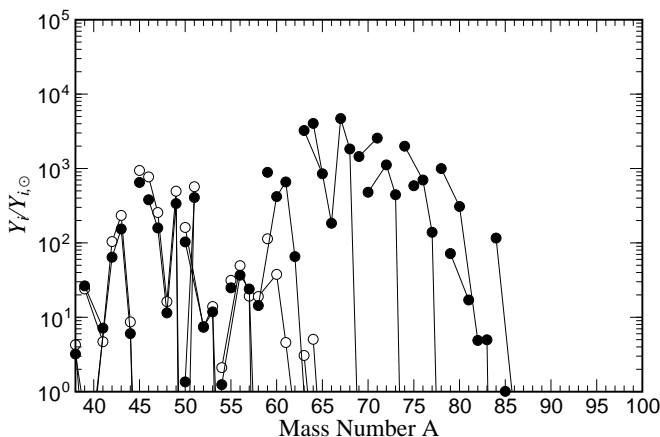


FIG. 7: Same as Fig. 3, but for model A5.

larger the fraction of free protons which are available per seed nucleus. To study the influence of entropy on the final nucleosynthesis abundances we have repeated the parameter study of model A1, however, replacing the entropy of the ejected matter by a smaller value ( $15 k_B$ , model A3) and by a larger value ( $50 k_B$ , model A4) than used in model A1 ( $30 k_B$ ). We mention again that the neutrino fluxes are the same in models A1, A3, and A4. The fact that for model A3 ( $15 k_B$ ), with lower entropy, there are less free protons available per seed nuclei translates into a smaller supply of neutrons produced by antineutrino captures and a less pronounced  $\nu p$ -process as observed for model A1. The behavior is opposite for model A4 ( $50 k_B$ ), where the larger entropy results in more free protons per seed nucleus, and consequently more free neutrons per seed, than model A1. These observations are confirmed by the abundance distributions shown in Figs. 5 and 6. Model A4 ( $50 k_B$ ) indeed shows a substantial amount of elements in the mass range  $A \sim 60 - 100$ , while model A3 ( $15 k_B$ ) produces only nuclides up to mass  $A \approx 80$  in a noticeably weaker  $\nu p$ -process.

As mentioned before, the disks have regions of differ-

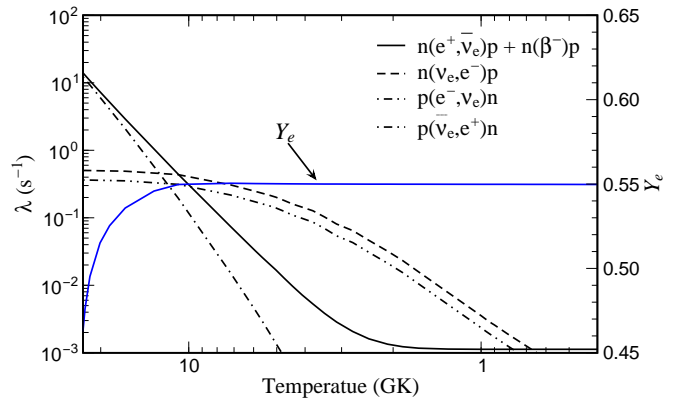


FIG. 8: (Color online) Same as Fig. 2, but for model A6.

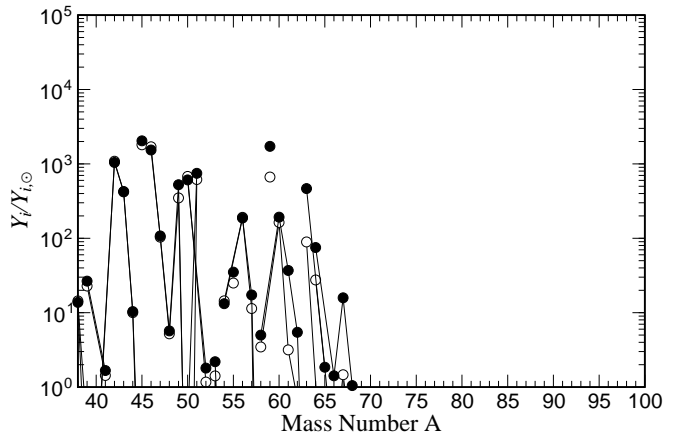


FIG. 9: Same as Fig. 3, but for model A6.

ent nuclear composition, density and temperature. The weak interaction rates in the outflows depend on the neutrino and antineutrino fluxes originating from the disk. The flux magnitudes in turn reflect disk conditions at certain radii. Thus the radius  $R_0$ , at which matter is released from the disk, affects  $\nu p$ -process nucleosynthesis as weak interaction rates in the outflow depend on the magnitude of the neutrino and antineutrino fluxes. In disks with comparable accretion rate at larger radii neutrinos will drive the composition less proton-rich as due to disk composition the neutrino fluxes are smaller. At smaller radii neutrinos will drive the composition more proton-rich and neutrino fluxes are larger.

To demonstrate this quantitatively we have repeated the nucleosynthesis calculation of model A4, however, replacing the radius at which matter is released to a larger value of  $R_0 = 250$  km (model A5). As expected, a weaker  $\nu p$ -process occurs in model A5 (Fig. 7).

Model A6 is the same as model A1, except that the matter accretion rate is significantly lower,  $\dot{M} = 0.1 M_\odot s^{-1}$  rather than  $1 M_\odot s^{-1}$  as assumed in all other models. As is explained in [14] this change in accretion rate has significant effects on the (anti-)neutrino surfaces. Consequently it also strongly affects the neutrino and antineu-

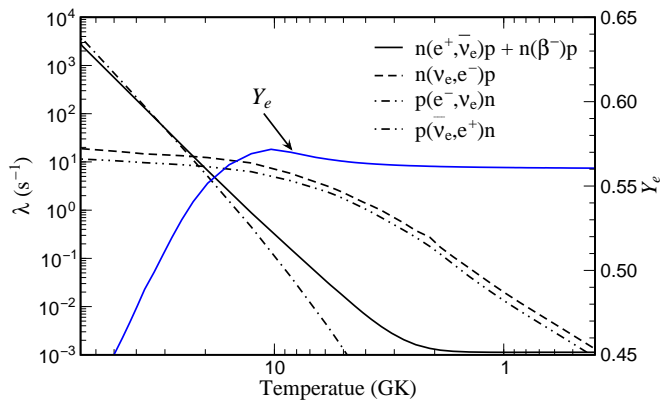


FIG. 10: (Color online) Same as Fig. 2, but for model B1.

trino fluxes which now are quite similar rather than dominated by a much stronger neutrino than antineutrino flux as encountered in the other models. The fluxes are in overall a factor of magnitude smaller than in models with higher accretion rate. Although the average antineutrino energy is slightly larger than the average neutrino energy, it is not the neutrino capture reactions which drive the composition slightly proton-rich in this model (see Fig. 8) but positron captures on free neutrons. The rates for the discussed reactions (Eq. 1) depend on the temperature and density of the disk. In fact, in model A6 a sufficient amount of positrons is produced which drives reaction (1c) to the right and makes the ejected matter proton-rich, reaching  $Y_e$  values up to 0.55. As is explained for model A1, once nuclei can be formed all neutrons are blocked in  ${}^4\text{He}$  with some free protons left. The formation of  ${}^4\text{He}$  occurs before weak freeze out. However, this value for  $Y_e$  is significantly smaller than in model A1 ( $Y_e \sim 0.72$ ). This fact together with the smaller antineutrino fluxes results in a smaller production of neutrons per seed nuclei and a rather weak  $\nu p$ -process, as is demonstrated in Fig. 9.

We now switch to the nucleosynthesis studies for the outflows from the disk model of Chen and Beloborodov [19]. This model predicts neutrino fluxes and spectra which are quite distinct from those of the disk model of DiMatteo *et al.* [18]. The differing treatments of relativity and the microphysics of the two disk models results in markedly different disk temperature and density profiles, particularly in the innermost regions with the greatest neutrino emission. In the DiMatteo *et al.* disk model, the temperature and density rise more steeply with decreasing radius and the innermost regions are significantly hotter and denser than in the Chen and Beloborodov disk model, resulting in correspondingly higher neutrino emission.

To explore the impact of these differences on the nucleosynthesis we have performed nucleosynthesis studies for the Chen and Beloborodov model (called models B1-B4) using the same parameters for the mass accretion rate, the acceleration parameter, the decoupling radius,

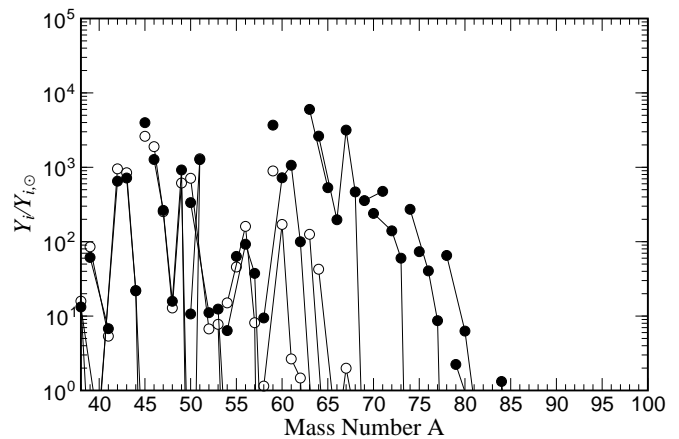


FIG. 11: Same as Fig. 3, but for model B1.

and the entropy as in models A1-A4 above (see Table I). Fig. 10 is the equivalent to Fig. 2 clearly showing impact of the different neutrino fluxes on the proton-to-neutron ratio of the ejected matter. In contrast to model A1, in which the neutrino luminosity exceeds the one for anti-neutrinos, by about an order of magnitude, the neutrino and anti-neutrino fluxes are rather similar in model B1. As a consequence also the neutrino and anti-neutrino capture rates on neutrons and protons, respectively, differ significantly less than in model A1. Moreover, neutrino and anti-neutrino capture rates are both smaller than the rates for positron and electron captures during the first second after matter has decoupled from the disk. This situation is similar to model A6, and again it is the slight dominance of positron over electron captures which drive the matter proton-rich at first. There is only a little time period in model B1 for which neutrino and anti-neutrino captures dominate the inverse weak-interaction processes. As the anti-neutrino capture rate is slightly larger by a factor of order 2, the ejected matter is further driven proton-rich during this short period. The final proton-to-neutron ratio  $Y_e = 0.56$  is much smaller than in model A1 ( $Y_e = 0.72$ ). We also observe an inverse alpha-effect in model B1, but it is milder than in model A1. Since  $Y_e > 0.5$ , the  $\nu p$ -process can also operate in model B1. However, its effectiveness is noticeably less than observed in model A1, as less free protons are available with a reduced antineutrino flux (see Fig. 11). While nuclides beyond  $A = 64$  are being made, the  $\nu p$ -process stops in model B1 already around  $A = 80$  and produces also smaller abundances of nuclides in the mass range  $A = 60 - 80$  than model A1.

Model B2 is the same as model B1, except that it has a smaller value for  $\beta$  (faster acceleration). Hence weak-interaction processes have less time to change the proton-to-neutron ratio. In fact, as can be seen in Fig. 12, the final value for  $Y_e$  is already been reached at a time of 0.1 s after the matter decoupled from the disk. More importantly for the nucleosynthesis, the value of  $Y_e$  stays below 0.5 in this model, i.e. the ejected matter is neutron-rich.

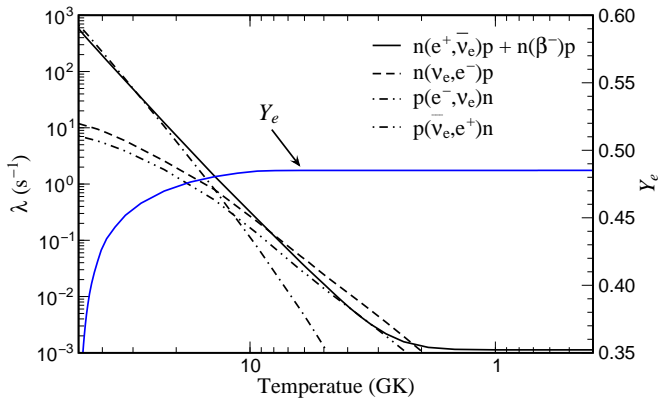


FIG. 12: (Color online) Same as Fig. 2, but for model B2.

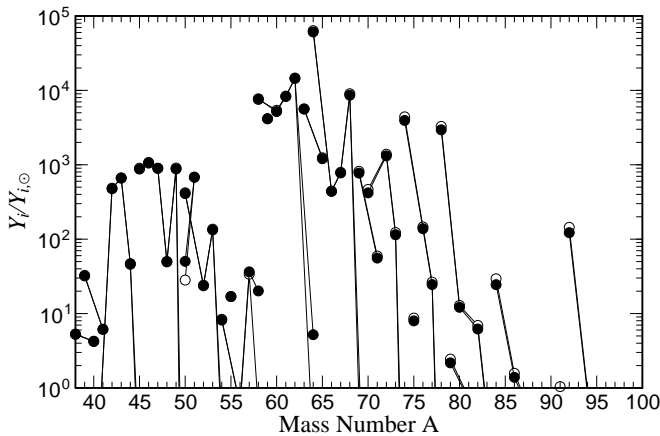


FIG. 13: Same as Fig.3, but for model B2.

We also observe that positron and electron captures dominate over neutrino and anti-neutrino captures during the time period in which the  $Y_e$  value of the ejected matter is set to its final value by weak interactions. With the matter being slightly neutron-rich, obviously no  $\nu p$ -process occurs. Fig. 13 shows that the abundance distributions are nearly identical with and without consideration of neutrino and anti-neutrino reactions in the nuclear network after the final  $Y_e$  value has been reached. These abundance distributions resemble those of an  $\alpha$ -process for a given value of  $Y_e < 0.5$ . The distinct differences in the abundance distributions of an alpha-rich freeze-out for proton-rich ( $Y_e > 0.5$ ) and neutron-rich ( $Y_e < 0.5$ ) matter is explained in [29].) We note that such an  $\alpha$ -process operates also in the neutrino-driven wind scenario setting up the abundance distribution for the seed nuclei of an subsequent r-process. However, in our model B2 the entropy is significantly smaller than required for successful r-process simulations in the neutrino-driven wind model. Due to this low entropy the neutron-to-seed ratio is too low in model B2 to allow for any r-process to occur. We note that the nuclear network considered in our nucleosynthesis studies is large enough to indicate potential r-process nucleosynthesis beyond the  $\alpha$ -process.

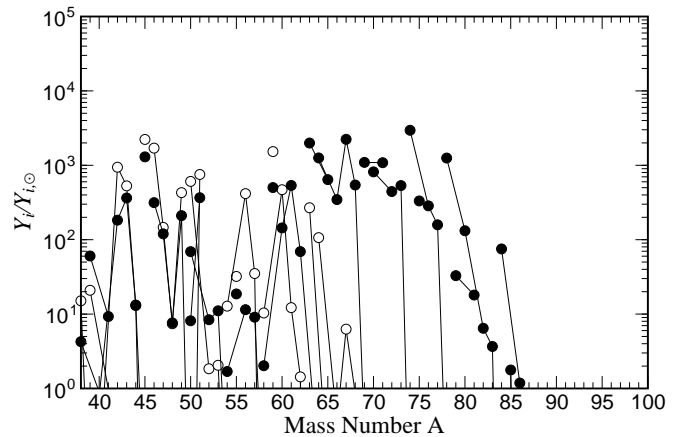


FIG. 14: Same as Fig. 3, but for model B3.

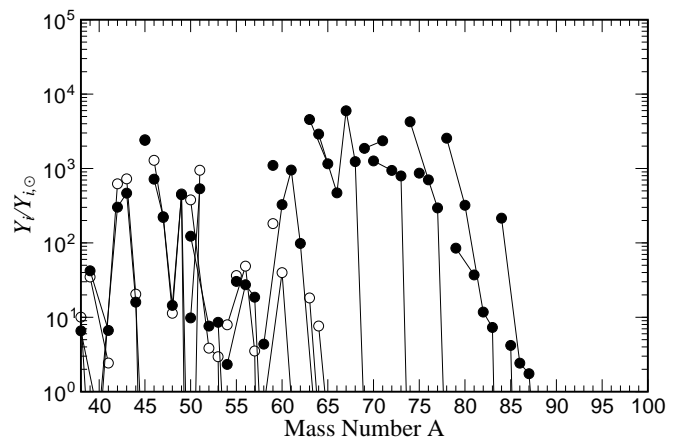


FIG. 15: Same as Fig. 3, but for model B4.

Models B3 and B4 are the same as model B1, however, assuming a smaller or larger value for the entropy ( $S = 15k_B$ , model B3 and  $S = 50k_B$ , model B4, respectively). As explained above, we expect a more pronounced  $\nu p$ -process to occur with growing entropy, as a larger amount of free protons (and hence neutrons after anti-neutrino captures) is available once heavy nuclei are being formed in the ejected matter. In fact, this is born out by our nucleosynthesis studies for models B3 and B4 (see Figs. 14 and 15), if compared to model B1. It is also interesting to compare the abundance results of models B3 and B4 to the equivalent studies of the DiMatteo *et al.* disk model (models A3 and A4). In both cases, the stronger  $\nu p$ -process nucleosynthesis occurs for the DiMatteo *et al.* disk models. The reason is the same as discussed in the comparison of models A1 and B1. The reduced enhancement of neutrino over anti-neutrino fluxes in the Chen and Beloborodov models translates into smaller  $Y_e$  values than in the corresponding DiMatteo *et al.* models. The consequence are smaller proton-to-seed (or neutron-to-seed) ratios available once the  $\nu p$ -process gets operable.

Finally, in model B5 we explore the effect of reducing

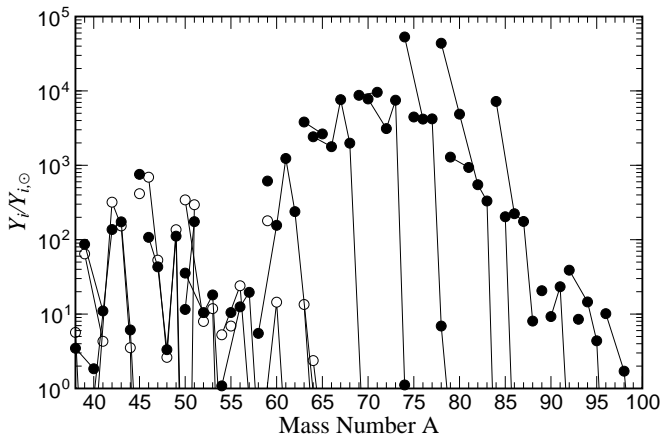


FIG. 16: Same as Fig. 3, but for model B5.

the radius  $R_0$  at which matter is released from the disk. This model is identical to B4, however, it uses a value for  $R_0$  of 50 km rather than 100 km. As discussed above, this change leads to an increase in the neutrino fluxes that will drive the composition more proton-rich and to a stronger  $\nu p$ -process. This expectation is indeed borne out in our calculations (see fig. 16), which shows noticeable strong production of elements with  $A > 75$ . In contrast to B4 (see fig. 15), model B5 synthesizes also elements in the mass range  $A = 90$ –100.

#### IV. CONCLUSIONS

Gamma-ray bursts are likely connected to an accretion disk surrounding a black hole. It has been found that the matter ejected from this disk can exhibit a rather rich range of nucleosynthesis [16] dependent on the matter accretion rate of the disk, the velocity and entropy of the outflow as well as the radius at which the matter is released. The composition of the outflow can be either neutron-rich, giving range to r-process like nucleosynthesis [14], or proton-rich. In this manuscript we have chosen the parameters characterizing the outflow such to focus on proton-rich nucleosynthesis and to investigate whether a  $\nu p$ -process can occur under reasonable conditions in the windlike outflows from a GRB accretion disk. This is indeed confirmed by our extensive nuclear network simulations. We find that it is essential to include neutrino capture interactions, particularly anti-neutrino capture on protons, when determining the nucleosynthetic outcomes for these environments.

In our present calculations, including disk models with accretion rates from  $0.1 M_\odot s^{-1}$  and  $1 M_\odot s^{-1}$ , we find that disk models with accretion rates of order  $1 M_\odot s^{-1}$  are particularly favorable for  $\nu p$ -process nucleosynthesis as these models exhibit significantly larger neutrino fluxes than antineutrino fluxes driving the matter proton-rich by a competition of neutrino captures on neutrons and antineutrino captures on protons. Our net-

work calculations show that for reasonable parameters describing velocity, entropy and ejection radius of the outflow a  $\nu p$ -process can occur which produces substantial abundances of nuclides up to the  $A \sim 100$  mass range. The effectiveness of the production in the mass range  $A \sim 60$ –100 depends somewhat on the entropy of the outflow; where larger entropies support a larger amount of free protons per seed nucleus and hence give a stronger  $\nu p$ -process as, by antineutrino capture, the free protons supply the neutrons for  $\nu p$ -process nucleosynthesis.

A crucial parameter for successful  $\nu p$ -process nucleosynthesis is the acceleration parameter  $\beta$  of the ejected matter as it defines the time matter is subjected to the neutrino interactions. Obviously the bigger the acceleration parameter, the more neutrino captures drive the matter proton-rich. Indeed by varying the acceleration parameter by a factor 3 we have demonstrated that the nucleosynthesis outcome can change from the occurrence of a strong  $\nu p$ -process to no  $\nu p$ -process nucleosynthesis. Slightly weaker (stronger)  $\nu p$ -process nucleosynthesis is also observed if the matter is released at larger (smaller) radii from the disk due to reduced (enhanced) neutrino capture rates.

It is also worth mentioning that our calculations show the occurrence of a process which in analogy to the alpha effect in r-process nucleosynthesis [7, 24, 25] we like to call “inverse” alpha effect. If the formation of  $^4\text{He}$ , which in proton-rich environment locks up all neutrons, occurs already before weak interaction freeze out, then continuous antineutrino capture on protons supply more neutrons, which combine with protons to build more  $^4\text{He}$ . This inverse alpha effect reduces the proton-to-neutron ratio in proton-rich environments (while in neutron-rich conditions it increases  $Y_e$ ). The inverse alpha effect is particularly important for outflows with rather slow acceleration parameters.

Accretion disk models are currently under development by several groups, so we have compared nucleosynthesis for the outflows of two different accretion-disk models. While we find the same basic conclusion: that the  $\nu p$ -process occurs, the details depend on the particular accretion disk model used. The model of DiMatteo *et al.* predicts a noticeable excess of neutrino flux over antineutrino flux. This difference is much milder in the disk model of Chen and Beloborodov. As a consequence of these differences in relative fluxes, the ejected matter in the disk model of Ref. [18] has always larger  $Y_e$  values than found for the model of [19]. Obviously the occurrence of an  $\nu p$ -process is always more pronounced for the former model if nucleosynthesis abundances are compared for the same values of mass accretion rate, matter acceleration, decoupling radii, and entropy. With the models A2 and B2 we have presented examples, where one disk model [18] predicts the occurrence of an  $\nu p$ -process, while, for the same parameter values, for the other [19] matter is ejected with a  $Y_e$  value less than 0.5 translating into an abundance distribution known from  $\alpha$ -rich freeze-out for neutron-rich matter.



In summary, within our parameter studies we have shown that outflow from accretion disks surrounding a black hole can be the site of  $\nu p$ -process nucleosynthesis. More quantitative studies of this exciting perspective have to wait until complete hydrodynamical simulations for the outflows from the accretion disks become available.

### Acknowledgments

We thank B. D. Metzger for useful discussions. The work of LTK, GMP and KL was partially supported by

the Helmholtz Alliance *Cosmic Matter in the Laboratory* and the Deutsche Forschungsgemeinschaft through contract SFB 634. This work was partially supported by the Department of Energy under contract DE-FG02-02ER41216 (GCM) and under contract DE-FG02-05ER41398 (RS).

- 
- [1] E. M. Burbidge, G. R. Burbidge, W. A. Fowler, and F. Hoyle, *Rev. Mod. Phys.* **29**, 547 (1957).
  - [2] A. G. W. Cameron, Report CRL-41, Chalk River (1957).
  - [3] G. Wallerstein, I. Iben, P. Parker, A. M. Boesgaard, G. M. Hale, A. E. Champagne, C. A. Barnes, F. Käppeler, V. V. Smith, R. D. Hoffman, et al., *Rev. Mod. Phys.* **69**, 995 (1997).
  - [4] M. Arnould, S. Goriely, and K. Takahashi, *Phys. Rep.* **450**, 97 (2007).
  - [5] M. Arnould and S. Goriely, *Phys. Rep.* **384**, 1 (2003).
  - [6] R. D. Hoffman, S. E. Woosley, G. M. Fuller, and B. S. Meyer, *Astrophys. J.* **460**, 478 (1996).
  - [7] G. M. Fuller and B. S. Meyer, *Astrophys. J.* **453**, 792 (1995).
  - [8] C. Fröhlich, G. Martínez-Pinedo, M. Liebendörfer, F.-K. Thielemann, E. Bravo, W. R. Hix, K. Langanke, and N. T. Zinner, *Phys. Rev. Lett.* **96**, 142502 (2006).
  - [9] J. Pruet, R. D. Hoffman, S. E. Woosley, H.-T. Janka, and R. Buras, *Astrophys. J.* **644**, 1028 (2006).
  - [10] S. Wanajo, *Astrophys. J.* **647**, 1323 (2006).
  - [11] A. I. MacFadyen and S. E. Woosley, *Astrophys. J.* **524**, 262 (1999).
  - [12] R. Surman and G. C. McLaughlin, *Astrophys. J.* **603**, 611 (2004).
  - [13] G. C. McLaughlin and R. Surman, *Phys. Rev. D* **75**, 023005 (2007).
  - [14] R. Surman and G. C. McLaughlin, *Astrophys. J.* **618**, 397 (2005).
  - [15] B. D. Metzger, A. L. Piro, and E. Quataert, *Mon. Not. Roy. Ast. Soc.* **390**, 781 (2008).
  - [16] R. Surman, G. C. McLaughlin, and W. R. Hix, *Astrophys. J.* **643**, 1057 (2006).
  - [17] R. Popham, S. E. Woosley, and C. Fryer, *Astrophys. J.* **518**, 356 (1999).
  - [18] T. Di Matteo, R. Perna, and R. Narayan, *Astrophys. J.* **579**, 706 (2002).
  - [19] W.-X. Chen and A. M. Beloborodov, *Astrophys. J.* **657**, 383 (2007).
  - [20] T. Rauscher and F.-K. Thielemann, *At. Data Nucl. Data Tables* **75**, 1 (2000).
  - [21] N. T. Zinner, Ph.D. thesis, University of Aarhus, Denmark (2007).
  - [22] W. R. Hix and B. S. Meyer, *Nucl. Phys. A* **777**, 188 (2006).
  - [23] W. R. Hix and F.-K. Thielemann, *J. Comput. Appl. Math.* **109**, 321 (1999).
  - [24] G. C. McLaughlin, G. M. Fuller, and J. R. Wilson, *Astrophys. J.* **472**, 440 (1996).
  - [25] B. S. Meyer, G. C. McLaughlin, and G. M. Fuller, *Phys. Rev. C* **58**, 3696 (1998).
  - [26] S. E. Woosley and R. D. Hoffman, *Astrophys. J.* **395**, 202 (1992).
  - [27] J. Witt, H.-T. Janka, and K. Takahashi, *Astron. & Astrophys.* **286**, 841 (1994).
  - [28] K. Lodders, *Astrophys. J.* **591**, 1220 (2003).
  - [29] I. R. Seitenzahl, F. X. Timmes, A. Marin-Lafleche, E. Brown, G. Magkotsios, and J. Truran, *Astrophys. J.* **685**, L129 (2008).